

## 水热纳米浇筑 HNTs 模板法制备碳纳米棒

刘 赞 刘盈盈 程志林\*

(扬州大学化学化工学院, 扬州 225002)

**摘要:** 以埃洛石纳米管(HNTs)为模板和聚乙烯醇(PVA)为碳源, 采用水热纳米浇筑法成功制备出碳纳米棒。方法涉及 3 步, 即在 HNTs 中浇筑 PVA, 碳化和模板移除。采用一系列表征手段如 XRD、FT-IR、SEM、TEM、Raman、XPS、SAED 和  $N_2$  吸附-脱附等表征碳纳米棒的形成和结构。具有一维棒状结构的碳纳米棒具有高的比表面积( $408\text{ m}^2\cdot\text{g}^{-1}$ )和典型的介孔特征。

**关键词:** 碳材料; 纳米棒; 埃洛石纳米管; 纳米浇筑

中图分类号: TB32 文献标识码: A 文章编号: 1001-4861(2017)04-0679-06

DOI: 10.11862/CJIC.2017.032

## HNTs-Templated Preparation of Carbon Nanorods by Hydrothermal Nanocasting Method

LIU Zan LIU Ying-Ying CHENG Zhi-Lin\*

(School of Chemistry and Chemical Engineering, Yangzhou University, Yangzhou, Jiangsu 225002, China)

**Abstract:** A novel method to prepare carbon nanorods through hydrothermal nanocasting method was presented using halloysite nanotubes (HNTs) as the template and polyvinyl alcohol (PVA) as the carbon source. This method involved in three steps, *i.e.* nanocasting PVA in HNTs, carbonization and etching removal of template. A series of characterization, such as XRD, FT-IR, SEM, TEM, Raman, XPS, SAED and  $N_2$  adsorption-desorption were used to detect the formation and structure of the as-prepared carbon nanorods (CNRs). The CNRs with a 1D rod-like structure were of high specific surface area ( $408\text{ m}^2\cdot\text{g}^{-1}$ ) and possessed typical mesoporous characterization.

**Keywords:** carbon materials; nanorods; halloysite nanotubes; nanocasting

### 0 Introduction

Carbon nanorods have attracted great interest from past few decades owing to their promising physical and chemical properties. The carbon nanorods are expected to have similar chemical properties of carbon nanotubes, which might find potential applications such as catalyst carriers<sup>[1]</sup>, electrodes<sup>[2]</sup> and composites<sup>[3]</sup>. To date, various methods have been demonstrated for the synthesis of carbon nanorods, which include the arc discharge method<sup>[4]</sup>, the chemical vapor deposition<sup>[5]</sup>,

the template methods<sup>[6]</sup>, the electron beam-induced route<sup>[7]</sup>, the reduction of carbon bisulfide<sup>[8]</sup> and the catalytic copyrolysis method<sup>[9]</sup>.

Recently, the templated synthesis via the nano-replication route appears to be a versatile method to build nanomaterials with high surface area and special porous nanostructure. Tang et al.<sup>[10]</sup> reported a modified nanocasting method to synthesize manganese oxide by SBA-15 template. The mixed oxide with a higher surface area exhibited a highest activity with 90% benzene conversion at  $250\text{ }^\circ\text{C}$  under a high space

收稿日期: 2016-10-19。收修改稿日期: 2016-12-06。

江苏省六大高峰人才计划(No.2014-XCL-013)资助项目。

\*通信联系人。E-mail: zlcheng224@126.com

velocity. Barrera et al.<sup>[11]</sup> synthesized nanostructured carbons by a nanocasting method, using a very ordered mesoporous material (SBA-15) as template and sucrose as carbon source. The final material consists of an ordered arrangement of parallel carbon nanorods bonded with some carbon nanowires (CMK-3 type), formed in the mesopores and micropores of the inorganic matrix.

Among other nanotemplates, halloysite nanotubes (HNTs) as naturally available aluminosilicate clay with *ca.* 15 nm in lumen diameter and 600~1500 nm in length, can become a promising candidate for nanoconfined template because of its well-defined hollow tubular structure, abundance in nature as a raw material, and the increasing demand for the environment-friendly products<sup>[12]</sup>. So far, it has been used for encapsulation and sustained-release of different chemical agents, such as proteins, drugs, antiseptics, antimicrobial agents, and corrosion inhibitors for metal protection<sup>[13-19]</sup>. Mu et al.<sup>[20]</sup> fabricated silver/halloysite nanotube/Fe<sub>3</sub>O<sub>4</sub> (Ag/HNT/Fe<sub>3</sub>O<sub>4</sub>) nanocomposites by selective modification of the lumen of halloysite nanotubes with silver nanorods and the external wall with Fe<sub>3</sub>O<sub>4</sub> nanoparticles, which exhibited an excellent catalytic activity and recyclability for the reduction of 4-nitrophenol to 4-aminophenol by NaBH<sub>4</sub>. Abdullayev et al.<sup>[21]</sup> synthesized silver nanorods inside the lumen of the halloysite by thermal decomposition of the silver acetate, which was loaded into halloysite from an aqueous solution by vacuum cycling.

Herein, we present a templated hydrothermal technique to prepare carbon nanorods (CNRs) employing halloysite nanotubes (HNTs) as template and polyvinyl alcohol (PVA) as carbon source. The formation and structure of as-prepared CNRs was determined by a series of characterizations.

## 1 Experimental

### 1.1 Synthesis of carbon nanorods

Before using, HNTs (200~500 nm in length and 15~25 nm in pore diameter, purchased from Golden Sun Ceramics Co., Ltd. in China) were calcined at 550 °C for 6 h in air, denoted HNT-550. 1.5 g of the

calcined HNTs was dried at 100 °C for at least 24 h in a drying oven. According to the  $m_{\text{PVA}}/m_{\text{HNTs}}$  of 2:1, HNTs powder were added into 15% PVA aqueous solution and stirred for 2 h. Then, the mixture solution was transferred into an autoclave and put into an oven to keep hydrothermal treatment at 180 °C for 18 h. After ending, the product was filtered and washed, denoted PVA-nanocasted HNTs. Subsequently, the above obtained product was carbonized at 700 °C for 3 h under N<sub>2</sub> atmosphere in a tube furnace, denoted C-nanocasted HNTs. Finally, the C-nanocasted HNTs were etched by 40% HF solution to remove the HNTs template completely. The insoluble solid was obtained, denoted CNRs.

### 1.2 Characterization

XRD patterns were obtained with D8 Advance X-ray diffraction in  $2\theta$  range of 5°~70° with operation condition at 40 kV and 30 mA (Cu K $\alpha$ ,  $\lambda=0.154$  nm). TEM images were recorded by Tecnai 12 transmission electron microscope. SEM images were recorded by S-4800 Scanning Electron Microscope (15 kV). XPS was recorded by ESCALAB 250Xi X-ray photoelectron spectrometer. Raman spectra were acquired on a Labram-1B (Dilor, France) confocal microscopy Raman spectrometer with a 532 nm wavelength incident laser light. N<sub>2</sub> adsorption-desorption isotherms were determined by using Sorptomatic 1990 Thermo Finnigen instrument.

## 2 Results and discussion

As shown in XRD patterns (Fig.1), the typical characteristic peaks of the calcined HNTs (Fig.1b) in  $2\theta$  range of =10°~23° have hardly disappeared, only existing the peak of quartz phase at 26.8°. This suggests that the crystal structure of the nanotube wall of HNTs was destroyed due to happening dehydration<sup>[22]</sup>. Compared to pure PVA and HNTs, the PVA-nanocasted HNTs (Fig.1d) have the main characteristic peaks at 12°, 19° and 26.6°, which contain the main feature peaks of pure HNTs and PVA. However, the feature peak at 12° should be assumed to the shift of the feature peak of pure PVA at 13°, hinting that it is likely to exist an interaction between PVA molecular

and the surface active group of HNTs in the PVA-nanocasted HNTs<sup>[23]</sup>. After carbonized at high temperature, the C-nanocasted HNTs are of the similar characteristic peaks with the calcined HNTs (Fig.1e). As shown in Fig.1f, the as-prepared CNRs have the feature peaks at  $25.5^\circ$  and  $44^\circ$ , which can be respectively indexed to (002) and (101) diffraction planes corresponding to the hexagonal graphite phase<sup>[24]</sup>. The two broadened peaks suggest the possible presence of an amorphous carbon phase within the as-prepared CNRs. No impurity in the as-prepared CNRs is observed in the XRD pattern.

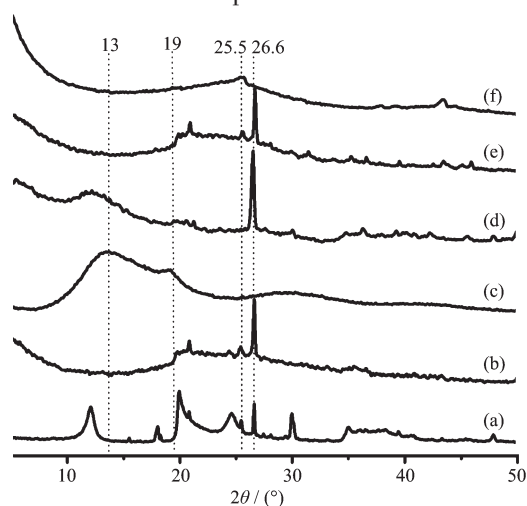


Fig.1 XRD patterns of HNTs (a), HNTs-550 (b), PVA (c), PVA-nanocasted HNTs (d), C-nanocasted HNTs (e) and as-prepared CNRs (f)

Fig.2 shows the FT-IR spectra of HNTs, PVA, PVA-nanocasted HNTs, C-nanocasted HNTs and as-prepared CNRs. As for the HNTs (Fig.2a), the peaks at  $3\,705$  and  $3\,621\text{ cm}^{-1}$  are assigned to the stretching vibrations of Al-OH groups at the surface of HNTs. The peaks at  $1\,650$  and  $1\,092\text{ cm}^{-1}$  are associated with the O-H bending vibration of water and the in-plane stretching vibrations of Si-O<sup>[25]</sup>, respectively. As shown in Fig.2b, PVA has the characteristic peaks at  $2\,943$  and  $2\,907\text{ cm}^{-1}$ , which should be ascribed to the C-H(CH<sub>2</sub>) asymmetric and symmetric stretching, respectively. Furthermore, there also are the peak at  $1\,437\text{ cm}^{-1}$  associated with the C-H(CH<sub>2</sub>) deformation vibration and the broad peak at  $3\,316\text{ cm}^{-1}$  assigned to -OH stretching vibration<sup>[26]</sup>. Compared to pure HNTs and PVA, the PVA-nanocasted HNTs contain the

main characteristic peaks of HNTs with PVA (Fig.2c). After carbonization at high temperature, the spectrum of the C-nanocasted HNTs have lost most of the characteristic peaks of pure HNTs and PVA, and only remain the feature peaks of Si-O groups (Fig.2d). No organic group originated from PVA is observed, indicating that the nanocasting PVA molecular was completely graphitized. The as-prepared CNRs possess the characteristic peaks at  $1\,161$  and  $1\,222\text{ cm}^{-1}$  associated with the C-O stretching vibration, and the peak at  $1\,564\text{ cm}^{-1}$  assigned to the C=C stretching vibration<sup>[27-29]</sup>. It indicates that the as-prepared CNRs materials have been successfully achieved by this method.

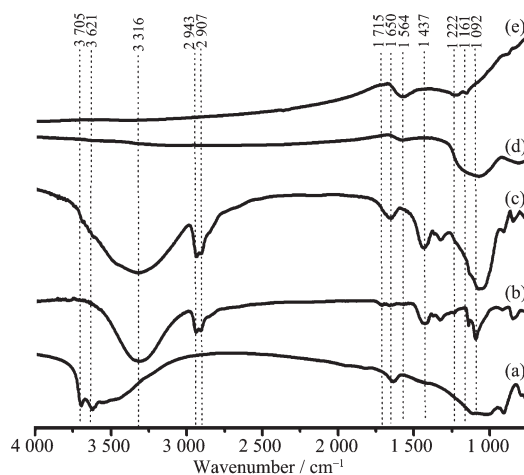


Fig.2 FT-IR spectra of HNTs (a), PVA (b), PVA-nanocasted HNTs (c), C-nanocasted HNTs (d) and as-prepared CNRs (e)

Fig.3 and Fig.4 display the SEM and TEM images of the products. The HNTs-550 still keep the hollow nanotube structure with *ca.* 20 nm in diameter and 200~1 000 nm in length (Fig.3a and Fig.4a). The SEM and TEM images of the PVA-nanocasted HNTs (Fig.3b and Fig.3b) show that PVA has successfully nanocasted in the hollow nanotube of HNTs. As shown in Fig.3c and Fig.4c~d, the carbon nanorods derived from the PVA-nanocasted HNTs can be clearly seen, indicating that the large quantity of the carbon nanorods with *ca.* 20 nm in diameter and 200~800 nm in length were obtained through this approach. The HRTEM and SAED images of the as-prepared CNRs. (Fig.4e,f) indicate that the as-prepared CNRs consist

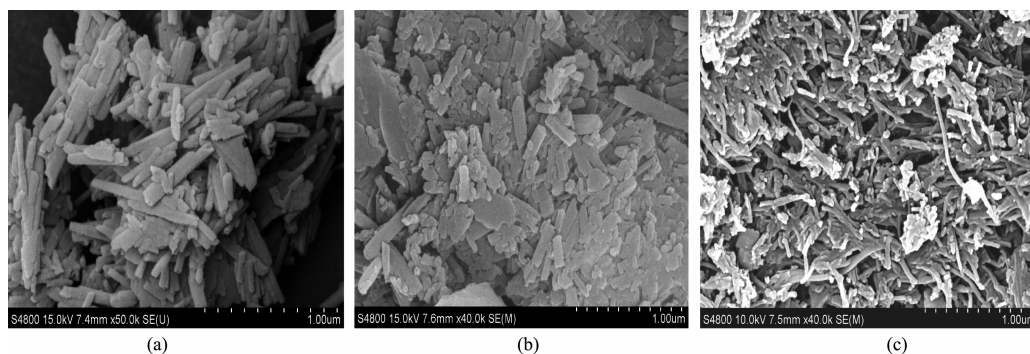


Fig.3 SEM images of HNTs (a), HNTs-550 (b) and as-prepared CNRs (c)

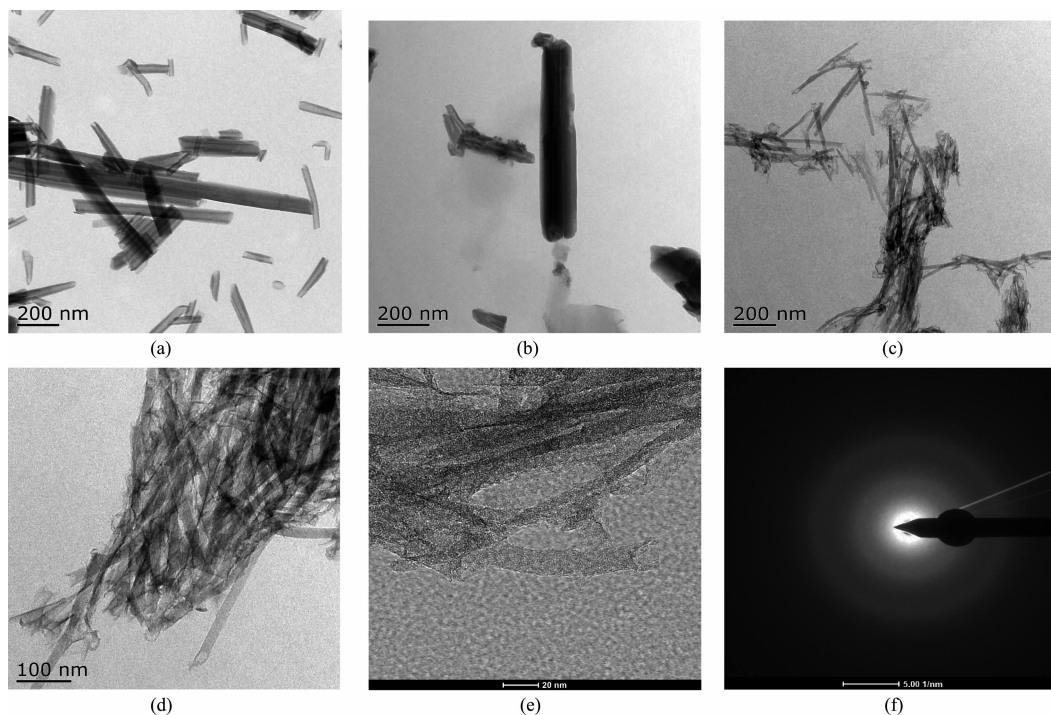


Fig.4 TEM images of HNTs (a), HNTs-550 (b), CNRs (c); HRTEM picture (h) and SAED pattern of as-prepared CNRs (i)

of the amorphous carbon nanoparticles.

The elemental composition of the as-prepared CNRs is determined by XPS as shown in Fig.5a. The as-prepared CNRs are composed of 91.5% C, 7.2% O and 1.3% S (atom ratio). The curve-fitting of C1s peak demonstrates the presence of bands at 284.8, 285.8, 287 and 288.4 eV, which are originated from graphitic carbon C-C/C=C, C-O, C=O and O-C=O, respectively<sup>[30]</sup>. As shown in Fig.5b, the as-prepared CNRs exhibited a D band at around 1 352  $\text{cm}^{-1}$  and a G band at around 1 584  $\text{cm}^{-1}$  in Raman spectrum, which correspond to the graphitic  $sp^2$  carbon structure and the disordered structure in  $sp^2$ -hybridized carbon system<sup>[31]</sup>. Moreover, the  $I_D/I_G$  value of the as-prepared CNRs is 0.75, indi-

cating that as-prepared CNRs have a higher graphitization degree and the fewer defects<sup>[32]</sup>.

The nitrogen adsorption-desorption isotherm and pore-size distribution of the products are shown in Fig.6. As shown in Fig.6(left), the isotherms of the as-prepared CNRs show a type IV isotherm and type H3 hysteresis loops<sup>[24]</sup>. In addition, the appearance of hysteresis loops at relative pressure higher than 0.45 indicates that the as-prepared CNRs are of the mesoporous structure<sup>[33]</sup>. The BET specific surface area value of the as-prepared CNRs is up to 408  $\text{m}^2 \cdot \text{g}^{-1}$ . As shown in Fig.6 (right), the BJH pore-size distributions of C-nanocasted HNTs almost lose the hollow nanopore feature of HNTs, confirming that PVA molecular has



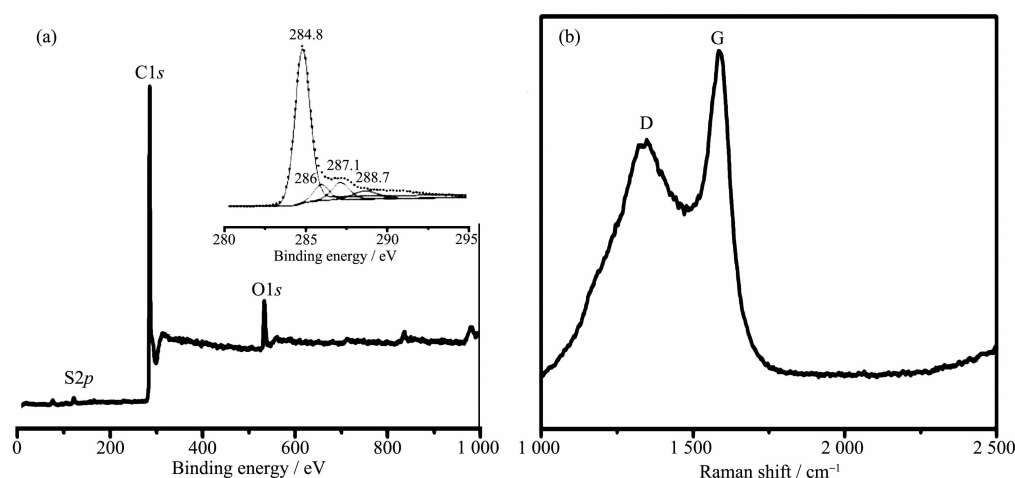


Fig.5 (a) Survey X-ray photoelectron spectrum and C1s spectrum (inset) of as-prepared CNRs; (b) Raman spectrum of as-prepared CNRs

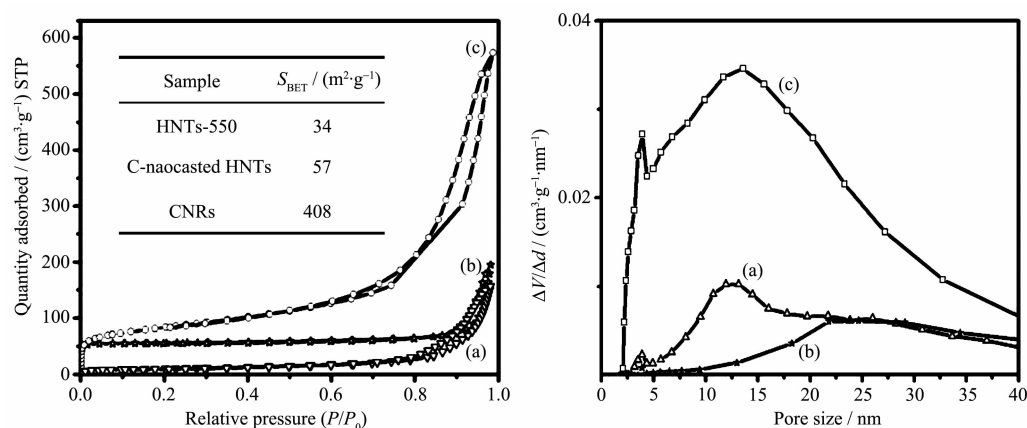


Fig.6  $N_2$  adsorption isotherms (left) and pore size distribution (right) of HNTs-550 (a), C-nanocasted HNTs (b) and as-prepared CNRs (c)

been successfully nanocasted in the nanotubes of HNTs by dipping method. In addition, it is also revealed that the as-prepared CNRs exist two types of the main mesopores at 3.9 and 13.5 nm, respectively.

### 3 Conclusions

The carbon nanorods were successfully synthesized by hydrothermal nanocasting method employing halloysite nanotubes (HNTs) as the template and polyvinyl alcohol (PVA) as the carbon source. The BET specific surface area value of the as-prepared CNRs was up to  $408 \text{ m}^2 \cdot \text{g}^{-1}$  and possessed two types of the mesopores at 3.9 nm and 13.5 nm.

**Acknowledgments:** This work was supported by the Talent Introduction Fund of Yangzhou University (2012), Key Research Project-Industry Foresight and General Key

Technology of Yangzhou (Grant No.YZ2015020), Innovative Talent Program of Green Yang Golden Phoenix (Grant No. yzlyjfh2015CX073), Yangzhou Social Development Project (Grant No.YZ2016072), Jiangsu Province Six Talent Peaks Project (Grant No.2014-XCL-013), Jiangsu Province Science and Technology Support Project (Grant No.BE2014613) and Jiangsu Industrial-academic-research Prospective Joint Project (Grant No.BY2016069-02). The data of this paper originated from the Test Center of Yangzhou University.

### References:

- [1] Patsalas P. *Thin Solid Films*, **2011**,**519**:3990-3996
- [2] Wang J, Chen Y, Zhang Y, et al. *J. Mater. Chem.*, **2011**,**21**: 18195-18198
- [3] Fan Y R, Zhao Z B, Zhou Q, et al. *Carbon*, **2013**,**58**:128-133
- [4] Liu Y Q, Hu W P, Wang X B, et al. *Chem. Phys. Lett.*, **2000**, **331**:31-34

- [5] Thien-Nga L, Hernadi K, Forro L. *Adv. Mater.*, **2001**,**13**:148-150
- [6] Kleitz F, Choi S H, Ryoo R. *Chem. Commun.*, **2003**,**9**:2136-2137
- [7] Chen K, Wu C, Hwang J S, et al. *J. Phys. Chem. Solids*, **2001**,**62**:1561-1565
- [8] Lou Z, He M, Zhao D, et al. *J. Alloys Compd.*, **2010**,**507**:38-41
- [9] Zou G, Lu J, Wang D, et al. *Inorg. Chem.*, **2004**,**43**:5432-5435
- [10] Tang W, Li J, Wu X, et al. *Catal. Today*, **2015**,**258**:148-155
- [11] Barrera D, Dávila M, Cornette V, et al. *Microporous Mesoporous Mater.*, **2013**,**180**:71-78
- [12] Yah W O, Xu H, Soejima H, et al. *J. Am. Chem. Soc.*, **2012**,**134**:12134-12137
- [13] Lvov Y M, Shchukin D G, Möhwald H, et al. *ACS Nano*, **2008**,**2**:814-820
- [14] Abdullayev E, Price R, Shchukin D, et al. *ACS Appl. Mater. Interface*, **2009**,**1**:1437-1443
- [15] Zhai R, Zhang B, Liu L, et al. *Catal. Commun.*, **2010**,**12**:259-263
- [16] Yuan P, Southon P, Liu Z, et al. *J. Phys. Chem. C*, **2008**,**112**:15742-15751
- [17] Abdullayev E, Lvov Y. *J. Mater. Chem.*, **2010**,**20**:6681-6687
- [18] Zhai H, Sun D, Wang H. *J. Nanosci. Nanotechnol.*, **2006**,**6**:1968-1792
- [19] Lin C, Danaie M, Liu Y, et al. *J. Nanosci. Nanotechnol.*, **2009**,**9**:4985-4987
- [20] Mu B, Wang W, Zhang J, et al. *RSC Adv.*, **2014**,**4**:39439-39445
- [21] Abdullayev E, Sakakibara K, Okamoto K, et al. *ACS Appl. Mater. Interface*, **2011**,**3**:4040-4046
- [22] Du Y, Zheng P. *Korean J. Chem. Eng.*, **2014**,**31**:2051-2056
- [23] Lee I W, Li J, Chen X, et al. *J. Appl. Polym. Sci.*, **2015**,**133**:42900-42911
- [24] Zheng R, Mo Z, Liao S, et al. *Carbon*, **2014**,**69**:132-141
- [25] Wang L, Chen J, Ge L, et al. *Energy Fuels*, **2011**,**25**:3408-3416
- [26] Swapna V P, Selvin T P, Suresh K I, et al. *Int. J. Plast. Technol.*, **2015**,**19**:124-136
- [27] Yu H. *J. Mater. Chem. A*, **2013**,**1**:12198-12205
- [28] Sha J, Li G, Chen X, et al. *Polym. Compos.*, **2016**,**37**:870-880
- [29] Wei Y, Ling X, Zou L, et al. *Colloids Surf. A*, **2015**,**482**:507-513
- [30] Zhang Z, Pfefferle L, Lhaller G. *Chin. J. Catal.*, **2014**,**35**(6):856-863
- [31] Kucukayan G, Ovali R, Ilday S, et al. *Carbon*, **2011**,**49**:508-517
- [32] Xu X, Lu Z, Hima H I, et al. *Appl. Clay Sci.*, **2009**,**42**:405-409
- [33] Jiang J, Chen Z, Duanmu C, et al. *Mater. Lett.*, **2014**,**132**:425-427
- [33] Wang A, Kang F, Huang Z. *Microporous Mesoporous Mater.*, **2008**,**108**:318-324